INVITED PAPER *Special Section on Terahertz Waves Coming to the Real World*

Towards MMIC-Based 300 GHz Indoor Wireless Communication Systems

Ingmar KALLFASS[†a)], **Iulia DAN**[†], **Sebastian REY**[††], **Parisa HARATI**[†], **Jochen ANTES**[†], **Axel TESSMANN**[†††], **Sandrine WAGNER**[†††], **Michael KURI**[†††], **Rainer WEBER**[†††], **Hermann MASSLER**[†††], **Arnulf LEUTHER**[†††], **Thomas MERKLE**[†††], ***and*** **Thomas KÜRNER**[††], ***Nonmembers***

SUMMARY This contribution presents a full MMIC chip set, transmit and receive RF frontend and data transmission experiments at a carrier frequency of 300 GHz and with data rates of up to 64 Gbit/s. The radio is dedicated to future high data rate indoor wireless communication, serving application scenarios such as smart offices, data centers and home theaters. The paper reviews the underlying high speed transistor and MMIC process, the performance of the quadrature transmitter and receiver, as well as the local oscillator generation by means of frequency multiplication. Initial transmission experiments in a single-input single-output setup and zero-IF transmit and receive scheme achieve up to 64 Gbit/s data rates with QPSK modulation. The paper discusses the current performance limitations of the RF frontend and will outline paths for improvements in view of achieving 100 Gbit/s capability.

key words: *THz communication, 300 GHz, MMIC*

1. Introduction

The rapidly growing interest in Terahertz (THz) wireless communication is fueled by the continued increase in global data traffic. This trend results in the need for massive data rate enhancement in all branches of the information and communication infrastructure, from the backbone network to the end user devices. The high available bandwidth, both in technical and in regulatory terms, coupled to the performance enhancements of modern semiconductor technologies, motivates the implementation of transmit and receive frontends operating at and above 300 GHz, a frequency range commonly referred to as "Terahertz", or, strictly speaking, the sub-millimeter wave frequency range. Due to the enormous free space path loss and the limited transmit power from solid-state electronic and photonic sources at such elevated frequencies THz wireless communication links are highly directive, as soon as distances of a few meter up to hundreds of meters are required. A wealth of applications is awaiting the technologies capable of realizing THz communication links with reasonable size and weight factors and in a commercially viable fashion. Among the most prospective applications of THz links are front- and backhauling of base stations in urban pico- and femto cells for highly directive, long range links of up to several hundreds of meters, reconfigurable links in smart office, data center and home theatre scenarios for medium transmission ranges on the order of tens of meters, and small range transmission below one meter in data kiosks and machine-to-machine communication.

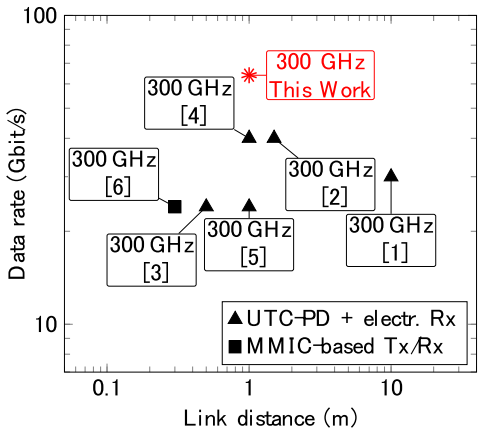

Fig. 1 Reported data rates and distances for wireless links operating at carrier frequencies at or above 300 GHz.

Very impressive results have been demonstrated using radio frontends implemented in photonic and active electronic technologies [1]–[6]. Based on an Indium-Phosphide (InP) double hetero-junction bipolar transistor (DHBT), [7] showed a transmission of 50 Gbit/s in an on-chip back-to-back setup. In [8], an InP DHBT fully integrated 300 GHz transceiver MMIC is presented. In previous work our group has demonstrated the transmission of 64 Gbit/s over 850 m [9] and 96 Gbit/s over 6 m [10] using a 240 GHz carrier frequency and an MMIC frontend based on GaAs metamorphic high electron mobility transistor (mHEMT) technology. Figure 1 illustrates the state of the art in submillimeter-wave wireless links, operating at or above a carrier frequency of 300 GHz, and employing both opto-electrical and pure electrical signal generation.

In this paper, we report on a 64 Gbit/s point-to-point link operating at a center frequency of 300 GHz, using highly integrated transmit and receive MMICs. The chip set is realized in a GaAs-based 35 nm mHEMT technology and associated MMIC process [11]. The transistors achieve cutoff frequencies f_T and f_{max} of more than 500 GHz and 1000 GHz, respectively.

Manuscript received July 15, 2015.
Manuscript revised August 20, 2015.

[†]The authors are with University of Stuttgart, 70569 Stuttgart, Germany.
[††]The authors are with Technische Universität Braunschweig, Germany.
[†††]The authors are with Fraunhofer Institute for Applied Solid State Physics, 79108 Freiburg, Germany.
a) E-mail: ingmar.kallfass@ilh.uni-stuttgart.de

DOI: 10.1587/transele.E98.C.1081

2. Technology

Due to the outstanding low noise characteristics and excellent high frequency performance of high indium content channel HEMTs [12], [13], they were the technology of choice for the implementation of the presented Rx and Tx MMICs. A metamorphic approach on 4″ semi insulating substrates is used for the epitaxial growth of the $In_{0.8}Ga_{0.2}As$/InAlAs device heterostructure. The lattice parameter of the GaAs substrate is transferred to that of InP by using a 1 μm thick quaternary InAlGaAs buffer layer.

Low resistance ohmic contacts, a 250 nm reduced gate-source distance and an optimized gate cross section are implemented in the process for an improved RF transistor performance. The PtTiPtAu gate as shown in Fig. 2 is defined with two separate electron beam lithography layers. In the first step a 35 nm PMMA 950 K resist opening is transferred in a SiN layer by dry etching. On top of the etched SiN trench, a 100 nm T-gate is defined in a three layer PMMA resist stack with an overlay accuracy better than 30 nm. During the gate evaporation, after recess etching, the SiN opening acts as a shadow mask for the metal. The gate is encapsulated in low-k BCB to reduce parasitic capacitances. An additional gate head is created by using the first metal interconnect layer on top of the e-beam written gate. This additional gate head reduces the gate line resistance which is important for high f_{max} and low noise figures. Some electrical transistor parameters are listed in Table 1.

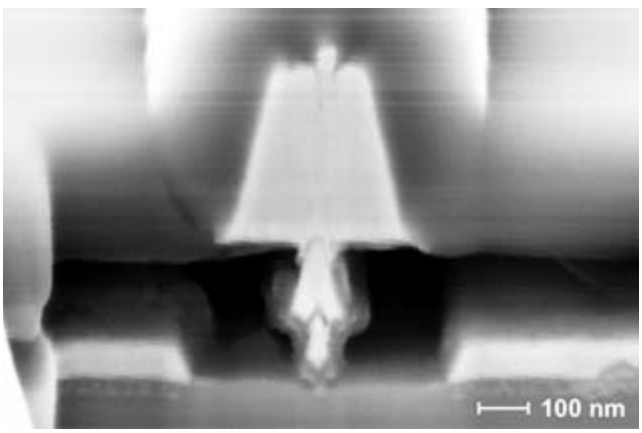

Fig. 2 SEM cross section of the 35 nm mHEMT gate

Table 1 Electrical parameters of the 35 nm mHEMT ($w_g = 2 \times 10\,\mu$m)

R_c	0.03 Ω·mm
R_s	0.1 Ω·mm
$I_{d,\,max}$	1600 mA/mm
V_{th}	-0.3 V
$BV_{off\text{-}state}$	2.0 V
$BV_{on\text{-}state}$	1.5 V
$g_{m,\,max}$	2500 mS/mm
f_T	515 GHz
f_{max}	> 1000 GHz

With increasing operating frequency and complexity of the MMICs the passive elements become more important. The technology provides up to four separate interconnection metal layers, 50 Ω/sq thin film resistors and MIM capacitors. The interconnect layers are separated by BCB, except the 2.7 μm thick Au plated top layer that realizes an air bridge technology. The sheet resistances of the metal layers are 0.8, 0.1, 0.1 and 0.008 Ω/sq, respectively.

To suppress substrate modes, the 4″ wafers are thinned down to a substrate thickness of 50 μm. Through-substrate vias are dry etched and the wafers are gold plated on the backside. An additional backside lithographic layer allows wet etching of the gold within the dicing streets. After on-wafer measurements, the 50 μm thick substrates are transferred on tapes and then they are laser diced to enable easy separation of multi project mask layouts. An automatic picking tool deposits the MMICs either in waffle packs or Gel-Paks®.

3. MMIC Chip Set

The analog frontend is built from three core MMICs: the transmitter (Tx), receiver (Rx) and local oscillator (LO) frequency multiplier (Fig. 3).

The Tx and Rx integrate a 300 GHz fundamental mixer, 100 to 300 GHz frequency tripler and 300 GHz RF post- and pre-amplifier stage, respectively. The LO frequency multiplier cascades three multiplication stages to provide a 100 GHz output from an 8.333 GHz input in X-band.

3.1 Transmit MMIC

Figure 4 shows the functional blocks of the transmit MMIC. The LO path consists of a frequency tripler from 100 to 300 GHz followed by a two-stage buffer amplifier. A single-balanced quadrature resistive FET mixer is used as an up-converter stage. The RF is post-amplified by a three-stage medium power amplifier, whose final stage uses a balanced

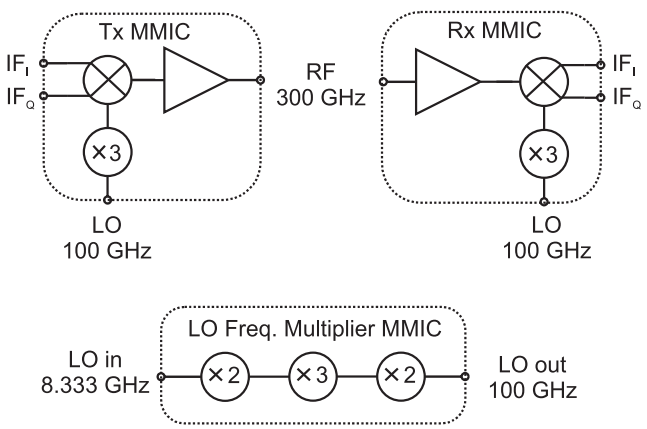

Fig. 3 MMIC chip set of the 300 GHz frontend.

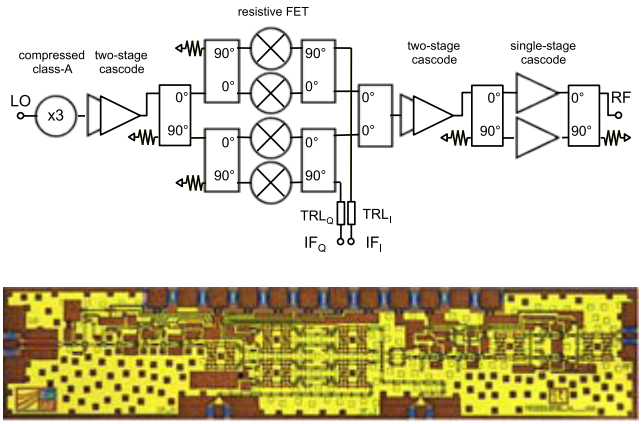

Fig. 4 Circuit architecture and chip photograph of the 300 GHz transmit MMIC. Chip size is $0.75 \times 3.25\,\text{mm}^2$.

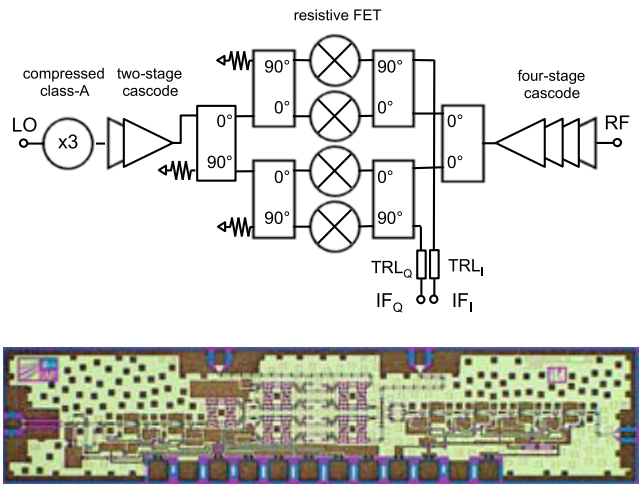

Fig. 5 Circuit architecture and chip photograph of the 300 GHz receive MMIC. Chip size is $0.75 \times 3.25\,\text{mm}^2$.

topology to combine the power of two parallel amplifier branches. All amplifier stages employ cascode gain cells. The 90° couplers in the mixer and power amplifier stages are implemented as tandem-X couplers, featuring a simulated operating frequency range from 280 to 360 GHz, an insertion loss of 1 dB and output port phase relation of 88° to 91° [14]. The couplers' isolated ports are terminated by integrated thin-film 50 Ω resistors, except for the couplers on the drain side of the resistive FET mixer cells, where the quadrature IF signals are applied. The equal length coplanar transmission lines TRL_I and TRL_Q preserve the phase balance of the IF signals and route the broadband signals to the contact pads of the mixer cells.

3.2 Receive MMIC

The receiver (Fig. 5) uses the identical sub-circuits for LO generation and mixing as the transmit MMIC. The single-balanced quadrature resistive FET mixer, now being used as a down-converter, is preceded by a four-stage low-noise

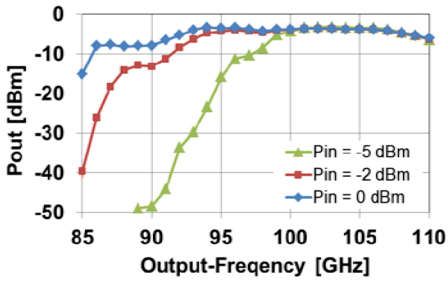

Fig. 6 Measured output power (Pout) as a function of the output frequency of the multiplier-by-12 MMIC, packaged in a waveguide module.

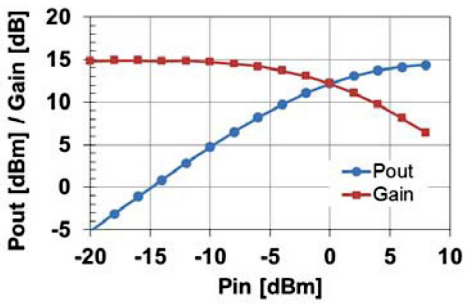

Fig. 7 Measured output power of the 100 GHz medium power amplifier, packaged in a waveguide module.

pre-amplifier stage in the receiver.

3.3 LO Frequency Multiplier

The Rx/Tx subharmonic LO signal of 100 GHz is generated by a broadband multiplier-by-12 MMIC (X12) similar to [15]. It is composed of a frequency doubler stage, followed by a tripler and another doubler stage. The center frequency of the designed MMIC is adjusted to 100 GHz corresponding to an input frequency of 8.333 GHz. The measured output power transfer characteristic of the packaged MMIC is depicted in Fig. 6 from 85 to 110 GHz for different input power levels. At an input power of 0 dBm, the X12 MMIC can be operated from 93 to 107 GHz with an output power of better than −4 dBm. The suppression of spurious harmonics is better than 40 dBc at 100 GHz, where the 11^{th} and 13^{th} harmonics are the most critical ones.

The output signal of the X12 MMIC is amplified by an additional broadband medium power amplifier MMIC to provide the required drive levels to the frequency triplers in the RX and TX MMICs. The measured output power and gain of the packaged amplifier MMIC at its center frequency of 100 GHz is depicted in Fig. 7. An output power of up to 15 dBm can be achieved. The gain-defined bandwidth is measured to be 20 GHz, compatible with the bandwidth of the X12 MMIC.

3.4 Waveguide Modules

All MMICs of the 300 GHz chip set are packaged in split-

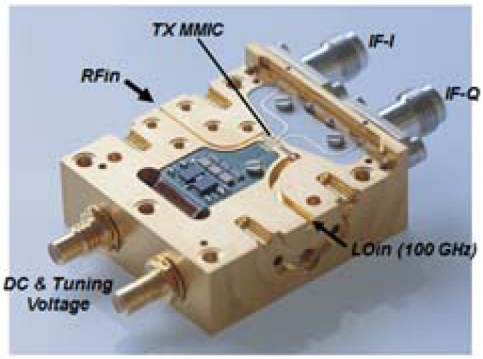

Fig. 8 Tx 300 GHz waveguide module. Depicted is one half of the split-block package.

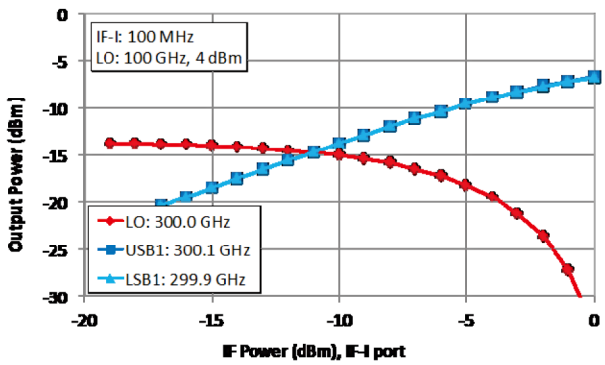

Fig. 9 Output power measurement of the Tx module measured using a calibrated spectrum analyzer with frequency extensions to H-band (220-330 GHz).

block waveguide modules. The MMIC-to-waveguide transitions are realized by quartz substrates, thinned down to the thickness of the MMICs, which is 50 μm. For this reason, ultra-short wedge-wedge bond wire connections can be placed between the MMIC bond pad and the microstrip transmission lines used on the quartz substrate. The rectangular waveguide mode is coupled by an E-plane probe to the microstrip mode. The insertion loss of a single transition is estimated to be better than 1.2 dB from 220-330 GHz [16].

The insight view of a 300 GHz Tx module is shown in Fig. 8. V-connectors and a liquid crystal polymer (LCP) substrate provide the Tx MMIC with the I and Q baseband data signals. A bandwidth of 50 GHz was measured for the IF path up to the MMIC. The LO (100 GHz) and RF signals (300 GHz) use a rectangular waveguide interface to connect to the X12 multiplier module respectively the transmit antenna.

The performance of the Rx and Tx MMICs packaged in the split block modules is characterized under continuous wave (CW) excitation. The presented results, summarized in Fig. 9 and Fig. 10, are obtained with a spectrum analyzer calibrated by power meter reference measurements. For the Tx module characterization, the spectrum analyzer operating frequency is extended by frequency extension modules. The power calibration refers the performance to the rectangular waveguide and V-connector interfaces, respectively. The LO signal at 100 GHz is provided by the X12 modules and the presented 100 GHz amplifier, also calibrated beforehand by power meter measurements.

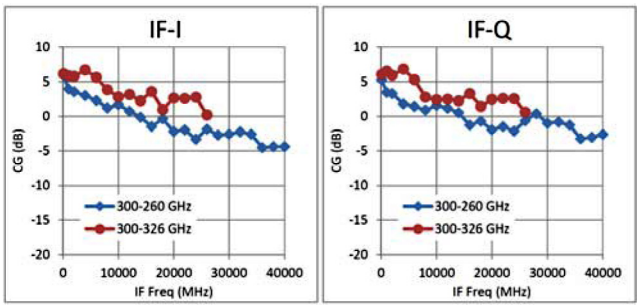

Fig. 10 Rx module conversion gain measurements.

The measured output power of the 300 GHz Tx module starts to saturate at −7 dBm. In this case, the IF frequency is set to 100 MHz. The lower and upper side bands are depicted for the case when the I-channel is used and the Q-channel is unconnected. The identical power levels are observed when the Q-channel is used and the I-channel is unconnected. The transmitted residual local oscillator power is less than −15 dBm in the operation region of interest which means when the IF power level exceeds −10 dBm.

The measured conversion gain (CG) of the Rx module has a linear slope of approximately 2.5 dB/10 GHz up to 40 GHz, both for the I and Q channel. Due to the waveguide band limit of the RF signal source at 325 GHz, the upper sideband cannot be fully characterized up to an IF frequency of 40 GHz. The I and Q channel performance agrees very well within the measurement uncertainties. The almost constant gain slope of approx. 0.25 dB/GHz in the receiver conversion gain is mainly due to the frequency-dependent loss of the microstrip line on the quartz substrate forming the transition from the MMIC to the IF connectors (cp. Fig. 8). Note that an identical slope is expected in the Tx module. Together with the IQ phase and magnitude imbalance this frequency characteristic will limit the achievable baud rate and the use of multi-level amplitude modulation formats.

4. Performance Estimation

4.1 Link Budget

With the Tx module performance discussed above, a maximum transmit power of −7 dBm per sideband together with an effective IF-bandwidth of at least 32 GHz can be achieved with digital baseband equalization. The measured noise figure of the LNA itself is 6.5 dB with a small-signal gain of 25 dB [17]. The downconverter's conversion gain is approximately −19 dB. This results in an estimated receiver noise figure of 6.7 dB.

According to the link budget in Table 2, when using a pair of horn antennas with a measured gain of 24.2 dBi each, a signal with an RF bandwidth of 64 GHz can be transmitted

Table 2 Link budget parameters.

Parameter	Unit	Value	Comment
Center frequency	GHz	300	
RF Tx power	dBm	-4.0	From single-tone measurement, DSB transmission
Tx and Rx antenna gain	dBi	24.2	From antenna measurements
Tx and Rx antenna efficiency	%	50	
Link distance	m	1.0	Used in transmission experiments
Free-space path loss FSPL	dB	82.0	
Bandwidth	GHz	64	DSB transmission
Link margin	dB	4.0	e.g. for antenna misalignment
Rx input power	dBm	-65.8	
Rx antenna noise	K	1356	
Rx antenna temperature	K	290	
Rx noise figure	dB	6.7	
Carrier-to-noise ratio C/N	dB	17.6	
Max range @ C/N = 10 dB	m	2.4	

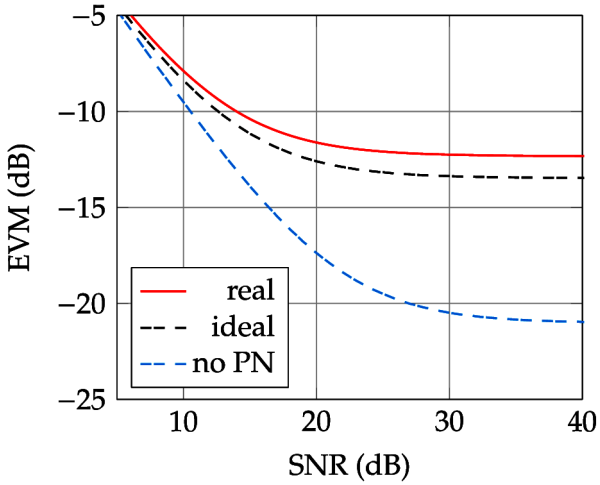

Fig. 11 Performance estimation of the 300 GHz link taking into account measured IQ imbalance and LO phase noise (“real”), ideal IQ balance (“ideal”) and zero LO phase noise (“no PN”).

over a distance of 2.4 m with a resulting SNR of approximately 10 dB.

4.2 Frontend Imperfections

Applying the theory developed in [18] to systems operating in the submillimeter-wave regime it can be shown that the accumulated phase error caused by the LO’s phase noise is the dominating signal distortion effect. The signal source used in the link setup shown here, provides a noise floor of better than −130 dBc/Hz at a frequency of 100 GHz. After the internal frequency multiplication by three, the noise floor seen by the mixer translates into −120.5 dBc/Hz. A phase error rms of 0.1342 rad can be calculated for a modulation bandwidth of 10 GHz.

The values for the I/Q-amplitude imbalance are obtained from the MMIC on-wafer measurements. The Tx shows an imbalance of 0.6 dB, averaged over a bandwidth of 10 GHz. The Rx imbalance over the same bandwidth is measured to be 0.4 dB. A measurement of the I/Q-phase imbalance cannot be performed with the available measurement equipment. Therefore, the values for both the Tx and Rx phase imbalance are extracted from S-parameter measurements of the 90°-hybrid used to realize the quadrature up- and down-converters. This is a viable approach, since the hybrid is assumed to introduce the largest phase deviation.

Using the above frontend imperfections and the EVM estimation algorithms shown in [18], the expected performance of the 300 GHz wireless system can be evaluated. The results of this estimation in terms of EVM versus the SNR at the receiver are shown in Fig. 11. First, the measured MMIC performance is taken into account. To further determine the influence of the different imperfections, in a second approach ideal MMICs, i.e. without I/Q-imperfections are assumed and in the last one, the actual MMIC performance but with an ideal LO source, i.e. a source without phase noise, is considered. For all three cases, the EVM curve enters an error floor, for which even with increasing SNR the link performance remains nearly constant. This error floor is determined by the different imperfections. The EVM error floor without the presence of phase noise stems from the superposition of IQ phase and magnitude imbalance of the Tx and Rx modules. Without any imperfection of the analog frontend, the EVM in logarithmic terms would be equal to −SNR. From the difference between the curve with phase noise and no imperfection and the one without phase noise, it is obvious, that the system performance is dominated by the LO phase noise. Even if a redesign of the Tx and Rx MMICs would result in perfect I/Q-balance, only marginally system improvement would be achieved. Also, Fig. 11 shows, that a SNR improvement due to a changed system setup or increased transmit power would not necessarily result in a better system performance. A more detailed analysis of the impact of different frontend imperfections on the link quality will be reported in [19].

5. 300 GHz Transmission

5.1 Link Setup

Figure 12 depicts the architecture of the realized 300 GHz wireless link experiment and the Tx and Rx analog frontend functional architecture. The LO-signal for the transmitter and receiver, i.e. the carrier frequency is generated by a highly stable signal synthesizer operating at 8.333 GHz. Employing a frequency multiplier chain with a multiplication factor of 36 translates the signal source’s output signal to the desired 300 GHz.

A state-of-the-art arbitrary waveform generator (AWG) with an analog bandwidth of 20 GHz and a sample rate of 65 GS/s is used to generate the in-phase (I) and quadrature (Q) input signals for the transmitter. Pseudo random

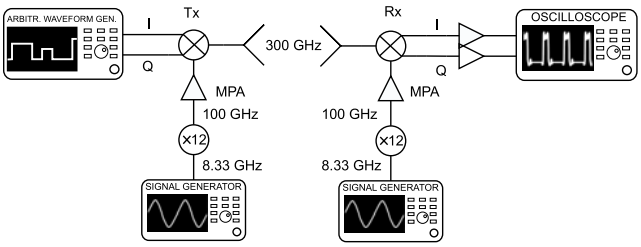

Fig. 12 Simplified block diagram of the 300 GHz radio link.

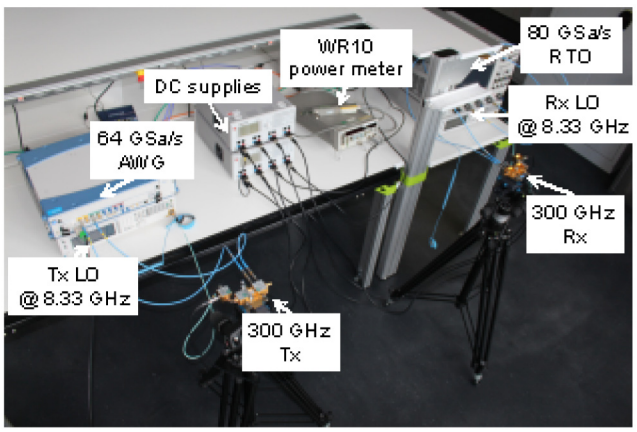

Fig. 13 Measurement setup of the 300 GHz wireless link.

binary sequences (PRBS) are used as test signals. At the receiver side, the down-converted signal is amplified by phase-matched baseband amplifiers and captured by a state-of-the-art real-time oscilloscope (RTO) featuring an analog bandwidth of 32 GHz together with a sampling rate of 80 GS/s. The necessary carrier recovery is realized in the digital domain by the use of Keysight's vector signal analyzer software (VSA). This software is also used to demodulate the signals and evaluate the frontend's performance in terms of error vector magnitude (EVM). The direct-conversion approach allows for a large IF-bandwidth and, together with quadrature up- and down-conversion, it is also capable of transmitting bandwidth-efficient complex modulated data signals.

Figure 13 shows the complete measurement setup used in the transmission experiments. Figure 14 shows the transmitter module chain in more detail. The LO signal at 8.333 GHz is fed to the multiplier module at a power level of −6.5 and −6.0 dBm at the Tx and Rx, respectively. To achieve the optimum drive power level for the transmit module, a medium power amplifier (MPA) and WR-10 waveguide attenuator are employed. A WR-10 power meter is used to adjust the LO power level to the optimum value of 4 dBm.

5.2 Receiver Sensitivity

In order to estimate the receiver sensitivity, an adjustable WR3 attenuator has been attached between the transmitter

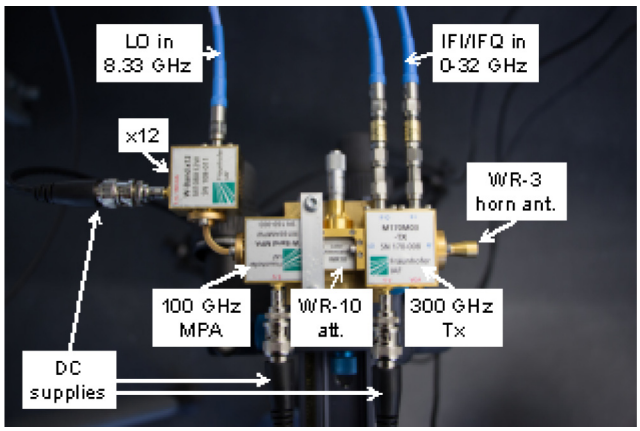

Fig. 14 Close-up of the transmitter module chain.

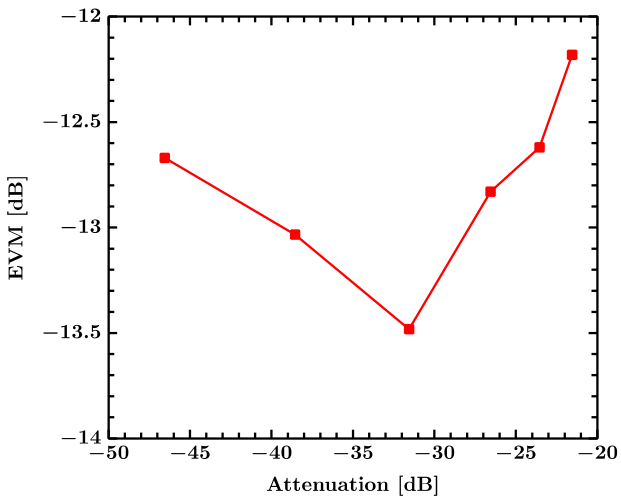

Fig. 15 Receiver sensitivity in terms of EVM versus attenuator setting for a 2 GBd QPSK transmission.

module and the antenna. For a distance of 0.25 m from the transmitter to the receiver the sensitivity in terms of EVM over the effective attenuation is depicted in Fig. 15 for a transmission of a QPSK signal with 2 GBd symbol rate. The effective attenuation is the sum of the antenna gains, the free space path loss and the additional attenuation from the waveguide attenuator. For higher attenuations the EVM increases because of the decreasing SNR, whereas for higher receive power levels the EVM increases due to nonlinearity effects. The optimum value of approx. 31.6 dB for the effective attenuation results from 70 dB of free space path loss, 2x24.2 dBi antenna gains and an additional attenuation of 10 dB. Assuming a total Tx power of −4 dBm by adding the power of both transmission sidebands (cp. Fig. 9), the corresponding optimum RF receive power is −35.8 dBm. Considering the single tone conversion gain of the Rx module, this value corresponds well to the total measured power of −27 dBm at the receiver's IF ports under optimum EVM conditions.

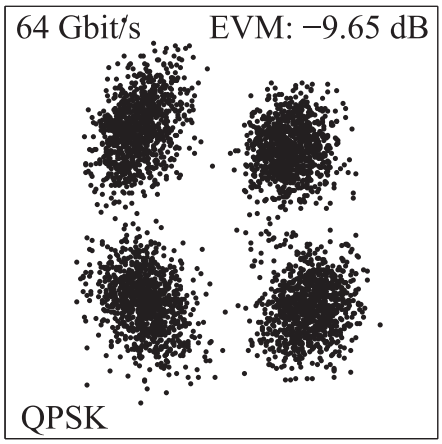

Fig. 16 Constellation diagram and EVM of the 1 m transmission of a 64 Gbit/s QPSK signal.

5.3 64 Gbit/s QPSK Transmission

Measurements have been performed for various combinations of symbol rates, modulation formats and distances. With only a simple equalization filter in the VSA software a maximum data rate of 64 Gbit/s has been demonstrated for a QPSK modulation at 32 Gbd. The scatterplot of the QPSK is presented in Fig. 16 for a distance of 1 m. Clearly the four constellation points can be distinguished from each other so that a demodulation is possible. The EVM value is −9.65 dB. Even for an increased distance of 2 m the demodulation has still been possible. The transmission distance is limited due to constraints in cable lengths in the experimental setup. The symbol rate is limited by the maximum rate of the AWG. Taking this into account even longer transmission distances, in the order of some meters, or higher data rates are possible. A further improvement in terms of data rate may be possible with higher order modulation schemes, which have been recorded but need to be assessed.

6. Discussion and Outlook

From the study of performance limitations due to frontend imperfections, we derive that the presented link is limited mostly by LO phase noise. This will be even more critical when the low phase noise synthesizers that were used in the experiments are replaced by custom 8.333 GHz phase locked loop (PLL) based oscillator boards. A revision of the optimum oscillation frequency and LO multiplication factor may become necessary.

Output power and linearity enhancements in the Tx will allow for higher complexity modulation formats, as well as more relaxed requirements on beam directivity or an increase in the transmission distance, depending on the target application scenario. Most applications will require some form of beam-steering, ideally by electronic means, but mechanically steered antennas may also be a viable option. For many applications, the employed waveguide packaging technology will be prohibitively expensive, and has too high form and weight factors. Replacing the waveguide modules by packaging solutions based on LTCC or softboard approaches, will be a major step towards commercially viable Terahertz communication systems. Finally, the challenges in power-efficient baseband electronics for the real-time transmission of user data at speeds of up to 100 Gbit/s are enormous and will require significant advances beyond today's state of the art in digital signal processing.

7. Conclusion

The presented transmission of 64 Gbit/s QPSK at a 300 GHz carrier frequency by means of a MMIC-based analog Tx and Rx frontend validates the applicability of microwave wireless communication techniques to the sub-millimeterwave regime, namely the implementation of electronic frequency generation, conversion and amplification. The approach offers one viable and scalable route towards Terahertz wireless communication systems.

Acknowledgments

This work was supported by the German Federal Ministry of Research and Education (BMBF) in the frame of the TERAPAN project under grant number 03V0563. We acknowledge the support of the Institut für Hochfrequenztechnik und Elektronik at Karlsruhe Institute of Technology in providing their high speed sampling oscilloscope to accomplish the transmission experiments.

References

[1] T. Nagatsuma, Y. Yoshimizu, Y. Yasuda, K. Oogimoto, S. Horiguchi, Y. Minamikata, and S. Hisatake, "30-gbit/s wireless transmission over 10 meters at 300 ghz," in Proc. 39th Int. Conf. on Infrared, Millimeter, and Terahertz waves (IRMMW-THz), pp.1–2, Sept. 2014.

[2] T. Nagatsuma and K. Kato, "Photonically-assisted 300-GHz wireless link for real-time 100-Gbit/s transmission," in Proc. IEEE MTT-S Int. Microwave Symposium (IMS), vol.1, no.4, pp.1–6, June 2014.

[3] H.-J. Song, K. Ajito, Y. Muramoto, A. Wakatsuki, T. Nagatsuma, and N. Kukutsu, "24 Gbit/s data transmission in 300 GHz band for future terahertz communications," Electronics Letters, vol.48, no.15, pp.953–954, July 19 2012.

[4] T. Nagatsuma, "Generating millimeter and terahertz waves by photonics for communications and sensing," in Proc. IEEE MTT-S Int. Microwave Symposium Digest (IMS), pp.1–3, June 2013.

[5] T. Nagatsuma, S. Horiguchi, Y. Minamikata, Y. Yoshimizu, S. Hisatake, S. Kuwano, N. Yoshimoto, J. Terada, and H. Takahashi, "Terahertz wireless communications based on photonics technologies," Opt. Express, vol.21, no.20, pp.23736–23747, 2013.

[6] H.-J. Song, J.-Y. Kim, K. Ajito, M. Yaita, and N. Kukutsu, "Fully integrated ask receiver mmic for terahertz communications at 300 ghz," IEEE Trans. on Terahertz Science and Technology, vol.3, no.4, pp.445–452, July 2013.

[7] H.-J. Song, J.-Y. Kim, K. Ajito, N. Kukutsu, and M. Yaita, "50-gb/s direct conversion qpsk modulator and demodulator mmics for terahertz communications at 300 ghz," IEEE Trans. on Microwave Theory and Techniques, vol.62, no.3, pp.600–609, March 2014.

[8] S. Kim, J. Yun, D. Yoon, M. Kim, J.-S. Rieh, M. Urteaga, and S. Jeon, "300 ghz integrated heterodyne receiver and transmitter with on-chip fundamental local oscillator and mixers," IEEE Trans. on Terahertz Science and Technology, vol.5, no.1, pp.92–101, Jan. 2015.

[9] I. Kallfass, F. Boes, T. Messinger, J. Antes, A. Inam, U. Lewark, A. Tessmann, and R. Henneberger, "64 gbit/s transmission over 850 m fixed wireless link at 240 ghz carrier frequency," Journal of Infrared Millimeter and Terahertz Waves, vol.36, no.2, pp.221–233, Feb. 2015.

[10] F. Boes, T. Messinger, J. Antes, D. Meier, A. Tessmann, A. Inam, and I. Kallfass, "Ultra-Broadband MMIC-Based Wireless Link at 240 GHz Enabled by 64 GS/s DAC," in Proc. 39th Int. Conf. on Infrared, Millimeter, and Terahertz Waves (IRMMW), Tuscon AZ, pp.1–4, Sept. 2014.

[11] A. Leuther, A. Tessmann, M. Dammann, H. Massler, M. Schlechtweg, and O. Ambacher, "35 nm mHEMT Technology for THz and ultra low noise applications," in Proc. 25th Int. Conf. on Indium Phosphide and Related Materials, Kobe, Japan, paper ThD2-2, May 2013.

[12] A. Leuther, A. Tessmann, P. Doria, M. Ohlrogge, M. Seelmann-Eggebert, H. Maßler, M. Schlechtweg, and O. Ambacher, "20 nm Metamorphic HEMT Technology for Terahertz Monolithic Integrated Circuits," in Proc. 9th European Microwave Integrated Circuit Conference, Rome, pp.84–87, 2014.

[13] X. Mei, W. Yoshida, M. Lange, J. Lee, J. Zhou, P.-H. Liu, K. Leong, A. Zamora, J. Padilla, S. Sarkozy, R. Lai, and W.R. Deal, "First Demonstration of Amplification at 1 THz Using 25-nm InP High Electron Mobility Transistor Process," IEEE Electron Device Lett., vol.36, no.4, pp.327–329, 2015.

[14] J. Antes, U. Lewark, A. Tessmann, A. Leuther, S. Wagner, and I. Kallfass, "Ultra-wideband single-balanced transmitter-mmic for future 300 ghz communication systems," in Proc. IEEE MTT-S Int. Microwave Symposium (IMS), Tampa, pp.1–3, June 2014.

[15] R. Weber, U. Lewark, A. Leuther, and I. Kallfass, "A W-band x12 multiplier MMIC with excellent spurious suppression," IEEE Microw. Compon. Lett., vol.21, no.4, pp.212–214, April 2011.

[16] A. Tessmann, A. Leuther, V. Hurm, H. Massler, S. Wagner, M. Kuri, M. Zink, M. Riessle, H.-P. Stulz, M. Schlechtweg, and O. Ambacher, "A broadband 220-320 GHz medium power amplifier module," in Proc. IEEE Compound Semiconductor Integrated Circuits Symposium (CSIC), La Jolla, pp.1–4, Oct. 2014.

[17] A. Tessmann, A. Leuther, H. Massler, M. Kuri, and R. Loesch, "A metamorphic 220-320 ghz hemt amplifier mmic," in Proc. IEEE Compound Semiconductor Integrated Circuits Symposium (CSIC), pp.1–4, Oct. 2008.

[18] Z. Chen and F.F. Dai, "Effects of LO Phase and Amplitude Imbalances and Phase Noise on M-QAM Transceiver Performance," IEEE Trans. Ind. Electron., vol.57, no.5, pp.1505–1517, 2010.

[19] J. Antes and I. Kallfass, "Performance estimation for broadband multi-gigabit millimeter and sub-millimeterwave wireless communication links," accepted for publication, IEEE Trans. Microwave Theory and Techniques, pp.1–13, 2015.

Ingmar Kallfass received the Dipl.-Ing. degree in Electrical Engineering from University of Stuttgart in 2000, and the Dr.-Ing. degree from University of Ulm in 2005. In 2001, he worked as a visiting researcher at the National University of Ireland, Dublin. In 2002, he joined the department of Electron Devices and Circuits of University of Ulm as a teaching and research assistant. In 2005, he joined the Fraunhofer Institute for Applied Solid-State Physics with a focus on nonlinear millimeter-wave integrated circuit design. From 2009 to 2012, he was a professor at the Karlsruhe Institute of Technology in the field of high-speed integrated circuits in a shared professorship with the Fraunhofer IAF in the frame of the German Excellence Initiative. Since 2013, he holds the chair for Robust Power Semiconductor Systems at the University of Stuttgart as part of the Robert Bosch Center for Power Electronics, where his major fields of research are compound semiconductor based circuits and systems for microwave and power electronics.

Iulia Georgiana Dan received the M.Sc. Degree in Electrical Engineering from the university of Stuttgart in 2015. Currently, she is pursuing her Ph.D. as a research assistant with the Institute of Robust Power Semiconductor Systems at the University of Stuttgart, with a focus on monolithic integrated circuit design for 300 GHz transceivers.

Sebastian Rey was born in Gifhorn, Germany, in 1982. He received the Dipl.-Ing. Degree in Electrical Engineering from the Technische Universität Braunschweig in 2012. Currently, he is pursuing his Ph.D. as a research assistant with the Institut für Nachrichtentechnik at Technische Universität Braunschweig. His research interests lies in the field of wireless communication systems at frequencies of 300 GHz and his work mainly focuses on propagation and system measurements and modeling. He is a contributor to IEEE 802.15.3d.

Parisa Harati received the Master of Science degree in Electrical Engineering from Technical University of Berlin in 2012 with the focus on mm-wave circuit design in CMOS technology. From 2013 she joined the IC design group in Heinrich Hertz Institute in Berlin, Germany and was engaged in design and characterization of modulator drivers in SiGe technology. She is currently a research assistant at the Institute of Robust Power Semiconductor Systems at the University of Stuttgart, working toward her Ph.D. degree with the focuse on mm-Wave Circuit Design and System simulation.

Jochen Antes received the Dipl.-Ing. degree in electrical engineering from the Karlsruhe In- stitute of Technology (KIT), Karlsruhe, Germany, in 2010. His diploma thesis, on the development of high-speed MMIC-based ac- tive frequency dividers, was carried out at the Fraunhofer Institute for Applied Solid- State Physics (IAF). From 2010 to 2013, he was with the Institut für Hochfrequenztechnik und Elektronik (IHE), KIT, as a research and teaching assistant. In 2013 he joined the Institute of Robust Power Semiconductor Systems (ILH) at the University of Stuttgart, Germany, where he is involved in the development of monolithic integrated circuits for broadband commu- nication systems. His research topics include high-speed mixed-signal millimeter- and sub-millimeter-wave circuit design and millimeter- wave wireless communication links.

Axel Tessmann received the Dipl.-Ing. and Ph.D. degrees in electrical engineering from the University of Karlsruhe, Karlsruhe, Germany, in 1997 and 2006, respectively. In 1997, he joined the High Frequency Devices and Circuits Department, Fraunhofer Institute for Applied Solid State Physics (IAF), Freiburg, Germany, where he is involved in the development of monolithically integrated circuits (ICs) and subsystems for high-resolution imaging systems and multi-gigabit wireless links. He is currently Group Leader of the Millimeter-Wave Packaging and Sub-System Group, IAF. His main research areas are the design and packaging of millimeter-wave and submillimeter-wave ICs using high electron-mobility transistors on GaAs, GaN, and InP, as well as circuit simulation and linear and nonlinear device modeling.

Sandrine Wagner received the Bachelor of Science degree in electronics and informatics from the University of Mulhouse, Mulhouse, France, in 1989. In 1989, she joined Micronas GmbH, Freiburg, Germany, where she was responsible for layout and physical verification of large-scale integrated semiconductor devices. In 2010, she joined the Fraunhofer Institute for Applied Solid State Physics (IAF), Freiburg, Germany.

Michael Kuri was born in Freiburg, Germany, in 1971. He received the diploma degree in Electrical Engineering from the University of Furtwangen, in 1996. From 1996 to 2000 he was with Storz, Kenzingen, Germany, where he was engaged in the design and routing of high-speed and high frequency digital and analog circuits. In 2000, he joined the High Frequency Devices and Circuits Department, Fraunhofer Institute for Applied Solid State Physics (IAF), Freiburg, Germany, where he is involved in the design, measurement and packaging of analog and digital ICs.

Rainer Weber was born in Offenburg, Germany, in 1978. He received the Dipl.-Ing. (FH) degree in Electrical Engineering from the University of Applied Sciences Offenburg, Germany, in 2003. He then joined the High Frequency Devices and Circuits Department of the Fraunhofer Institute for Applied Solid-State Physics (IAF), Freiburg, Germany, where he is involved in the MMIC design of amplifiers, oscillators, multipliers, and mixers up to 600 GHz.

Hermann Massler was born in Radolfzell, Germany, in 1965. He studied electrical engineering at the Technical University Karlsruhe where he graduated in 1993. While working on his diploma degree at the Forschungszentrum Karlsruhe (FZK) he performed and investigated quasi-optical measurements at 140 GHz. He continued these studies as a FZK Research Assistant for an additional year. Since 1994 he has been with the Fraunhofer Institute for Applied Solid State Physics (IAF) in Freiburg, Germany, working on transistor- and IC-characterization up to 1.1 THz.

Arnulf Leuther received the Dipl. Phys. degree and Ph.D. degree in physics from the Technical University of Aachen, Aachen, Germany. Since 1996, he has been with the Fraunhofer Institute for Applied Solid State Physics (IAF), Freiburg, Germany. His major research area is the development of HEMT technologies for sensor and communication systems up to 600 GHz.

Thomas Merkle received his M.Sc. degree from the University of Stuttgart, Germany, in 1999, and his Ph.D. degree from the University of Ilmenau, Germany, in 2006, all in electrical engineering. Upon completion of his M.Sc., he joined the Fraunhofer Institute for Applied Solid State Physics (IAF), Freiburg, Germany, where he worked in the field of nonlinear transistor modeling and design of MMICs up to 110 GHz. From 2005 to 2010, he was a Post-Doctoral Fellow at the CSIRO ICT Centre, Sydney, Australia, with focus on active integrated antennas for phased-array communication links at 71-86 GHz. From 2010 to 2013, he was a Senior Research Engineer at the Sony Technology Center in Germany, responsible for the design of sub-millimeter-wave MMICs and SiPs. In 2013, he returned to the Fraunhofer IAF. Currently he is a Project Manager and Senior Researcher in the area of integrated radar and wireless communication systems at 300 GHz and beyond.

Thomas Kürner received his Dipl.-Ing. degree in Electrical Engineering and his Dr.-Ing. degree from Universität Karlsruhe (Germany). From 1990 to 1994 he was with the Institut für Höchstfrequenztechnik und Elektronik (IHE) at the University of Karlsruhe. From 1994 to 2003, he was team manager radio network planning support at the the cellular operator E-Plus Mobilfunk GmbH &Co KG, Düsseldorf. Since 2003 he is Professor for Mobile Radio Systems at the TU Braunschweig. His working areas are propagation, traffic and mobility models for automatic planning of mobile radio networks, self-organization of cellular networks, car-to-x communications as well as indoor channel characterisation for high-speed short-range systems including future terahertz communication systems and accuracy of satellite navigation systems. Currently Thomas Kürner is the project coordinator of the German BMBF-VIP-TERPAN project on Terahertz Personal Area Network. At IEEE 802.15 he chairs the Task Group 3d, and the Interest Group THz.